Revista Brasileira de Ciência do Solo

Division - Soil in Space and Time | Commission - Pedometry

Satellite Spectral Data on the Quantification of Soil Particle Size from Different Geographic Regions

José Alexandre Melo Demattê[(1)*], Clécia Cristina Barbosa Guimarães[(2)], Caio Troula Fongaro[(2)], Emmily Larissa Felipe Vidoy[(3)], Veridiana Maria Sayão[(2)], André Carnieletto Dotto[(2)] and Natasha Valadares dos Santos[(2)]

[(1)] Universidade de São Paulo, Escola Superior de Agricultura "Luiz de Queiroz", Departamento de Ciência do Solo, Piracicaba, São Paulo, Brasil.
[(2)] Universidade de São Paulo, Escola Superior de Agricultura "Luiz de Queiroz", Departamento de Ciência do Solo, Programa de Pós-Graduação em Solos e Nutrição de Plantas, Piracicaba, São Paulo, Brasil.
[(3)] Universidade de São Paulo, Escola Superior de Agricultura "Luiz de Queiroz", Curso de Gestão Ambiental, Piracicaba, São Paulo, Brasil.

ABSTRACT: The study of soils, including their physical and chemical properties, is essential for agricultural management. Soil quality must be maintained to ensure sustainable production of food and conservation of natural resources. In this context, soil mapping is important to provide spatial information, which can be performed using remote sensing (RS) techniques. Modeling through use of satellite data is uncertain regarding the amplitude of replicability of the models. The aim of this study was to develop a quantification model for soil texture based on reflectance information from a continuum of bare soils, obtained by overlapping multi-temporal satellite images, and apply this model to an unknown region to evaluate its applicability. Spectral data were extracted from two Landsat TM 7 satellite images containing only bare soil, representing two distinct regions in Brazil (Area 1 and Area 2). The spectral data (obtained from six bands) and laboratory data (particle size from the 0.00-0.20 m layer) of Area 1 were modeled and extrapolated to Area 2. The bare soil images differentiated textural classes as sandy, sandy loam, clayey loam, clayey, and very clayey soil. The coefficients of determination between the determined and estimated values were higher than 0.5 and errors lower than 13 % for Area 1 and 30 % for Area 2, indicating applicability of the model to unknown areas.

Keywords: soil texture, remote sensing, bare soil mask, multiple linear regression, digital soil mapping.

*** Corresponding author:**
E-mail: jamdemat@usp.br

Received: December 6, 2017
Approved: April 3, 2018

How to cite: Demattê JAM, Guimarães CCB, Fongaro CT, Vidoy ELF, Sayão VM, Dotto AC, Santos NV. Satellite spectral data on the quantification of soil particle size from different geographic regions. Rev Bras Cienc Solo. 2018;42:e0170392. https://doi.org/10.1590/18069657rbcs20170392

INTRODUCTION

Soil quality plays a significant role in determining the nature of plant ecosystems and the capacity of the earth to sustain life, particularly human life (Brady and Weil, 2013). Demand for greater food production due to population increase has caused serious damage to the environment and thus to soils (Foley et al., 2005), such as deterioration of physical and chemical soil properties, causing land degradation (Li et al., 2009; Zeng et al., 2009). In this sense, knowledge of soil physical and chemical properties as well as of soil distribution on the earth's surface is essential for proper land use (Feizizadeh and Blaschke, 2013). These data can be obtained by conventional methods, as established by Teixeira et al. (2017), which can be laborious and time-consuming, or can be evaluated with the assistance of remote sensing (RS) techniques. The RS techniques are faster and less expensive and do not generate chemical residues or sample destruction (Okparanma and Mouazen, 2013).

The quantification of soil properties by RS started from the development of the Near Infrared Reflectance Analysis (NIRA) method, which used near infrared and shortwave data (Ben-Gera and Norris, 1968). This method assumes that the concentration of a component is proportional to the linear combination of several absorption factors. It presented a first calibration stage, where a prediction equation was developed based on analysis of multiple linear regression (MLR) between the chemical data and spectral bands and a second stage that comprised the validation of the method. The technique to the visible region was applied by Ben-Dor and Banin (1995) using laboratory data to simulate the bands of the Landsat satellite and managed to predict carbonate ($CaCO_3$) contents, specific surface area, total silica (SiO_2), and residual loss-on-ignition.

Soil texture, which includes sand, silt, and clay contents, is an important property for many soil functions, and other soil properties depend on soil texture. Soil structure, water retention capacity, aeration, organic matter content, susceptibility to erosion, cation exchange capacity, and others are influenced by soil texture, which is an indispensable property in soil classification systems (Hristov, 2013). In addition, soil texture is one of the most important factors in selection and growth of agricultural crops (Chakraborty and Mistri, 2015).

Many studies have used RS techniques for estimation of soil texture, with suitable results. Models of texture quantification were first developed with laboratory spectral data (Coleman et al., 1991). Spectral standards obtained in the laboratory allow us to understand satellite standards, since the concept of energy interaction is identical to what occurs in the laboratory, changing only the scale and configuration of the equipment. Therefore, studies have been conducted using laboratory data to simulate satellite data (Palacios-Orueta and Ustin, 1998) and they have reported the predictive capacity of the satellite data in relation to the proximal data (Coleman et al., 1993; Nanni and Demattê, 2006; Demattê et al., 2009).

From understanding of spectral behavior at the satellite level, new prediction models have been tested to improve their accuracy. Adjustments are required in the models and methods to improve spectral responses since spectral soil data coming from satellite are affected by atmospheric attenuations, increased signal-to-noise ratio, pixel size of images, soil cover, geometric view, and sensor spectral resolution. The soil surface texture was modeled by Liao et al. (2013) using stepwise multiple regression, kriging, and co-kriging; they found the best prediction by using the last method. Sand, silt, and clay contents were modeled by Chagas et al. (2016) using MLR and the Random Forest methods. These authors used all the bands of Landsat TM 5 and different indexes, which helped to identify bare soil, improving accuracy of the models. From this, it became clear that techniques that result in areas containing only bare soil are needed for better prediction of soil texture. In Brazil, Alves (2008) developed a method to detect

bare soil by using a single image, particularly through analysis of individual pixels and highlighted the usefulness of multi-temporal images for soil evaluation. Authors such as Demattê et al. (2016) and Fongaro (2015) upgraded the method by overlapping the multi-temporal images and visualizing an entire region containing only bare soil. This methodology is innovative and essential for soil studies, as texture changes gradually in the landscape.

Prediction models developed with the use of satellite sensors are calibrated based on local conditions, using small areas with low variation, and they do not allow application of these models to different study areas. This occurs because the spectral response behaves according to the interaction of electromagnetic energy with the components in the soil samples selected. Satellite images require the image pixels to be as pure as possible for the energy to interact only with the object under study. Energy absorption causes electronic transitions. Molecular vibrations are specific to samples, resulting in a standard spectral response for the samples selected.

The higher the sampling variability, the greater the chances of creating a model that can be extrapolated. The development of a prediction model that can be applied to different areas makes satellite RS an effective technique for agricultural management. The aim of this study was i) to develop a model of soil texture quantification from reflectance of a continuum of bare soils, obtained by overlapping multi-temporal satellite imagery (Fongaro, 2015) and ii) apply the model to unknown regions.

MATERIALS AND METHODS

Characterization of the study site

The steps of the methodology used are shown in figure 1. The study was conducted at two sites. The first was used to generate the model and is located in the northeastern region of the state of São Paulo, comprising 56 municipalities, with an area of approximately 14,600 km^2. The central point of the site is at 21° 49’ 53” S and 48° 7’ 5” W, Sirgas2000 projection system, 22/23 S zones. The climate of the region is Aw type (Köppen classification system), tropical with dry winters (Rolim et al., 2007), annual rainfall of 1,500 mm, and average annual temperature of 28 °C, where sugarcane cultivation predominates. Altitude ranges from 400 to 1,080 m. The geology consists of the Botucatu Formation, Pirambóia Formation, Serra Geral Formation, Itaqueri Formation, Marília Formation, Rio Peixe Valley Formation, Corumbataí Formation, alluvial deposits, colluvium and eluvial deposits, and detrital-lateritic covers (CPRM, 2006) (Figure 2). The soils are predominantly *Latossolos Vermelhos* and *Latossolos Vermelho-Amarelos*, with medium to silty texture, ferric or not; *Argissolos Vermelhos* and *Vermelho-Amarelos*, with variable texture and gradient; *Neossolos Quartzarênicos*; and *Nitossolos* [Ferralsols, Lixisols, Arenosols, and Nitisols, respectively (IUSS Working Group WRB, 2015)].

Area 2 was used for extrapolation/validation of the model. It is located between the states of Mato Grosso and Goiás and comprises six municipalities, with an approximate area of 5,000 km². The central point of the site is at 17° 43’ 40” S and 53° 18’ 3” W, Sirgas2000 projection system, 22 S zone. Climate data in the region were extracted from the New LocCim software 1.0 (Agrometeorology Group FAO) and obtained from the Embrapa website. Annual average temperature is 24 °C and annual rainfall is 1,490 mm, with predominance of sugarcane. The geology consists of the Aquidauana Formation, Cachoeirinha Formation, Corumbataí Formation, Irati Formation, Ponta Grossa Formation, Rio do Peixe Valley Formation, Serra Geral, Botucatu Formation, undifferentiated detrital covers and alluvial deposits (CPRM, 2004) (Figure 2). The soils that predominate in the region are *Latossolos Vermelhos*, *Latossolos Vermelho-Amarelos,* and *Neossolos Quartzarênicos* (SIEG, 2013); which correspond to a Ferralsols and Arenosols (IUSS Working Group WRB, 2015).

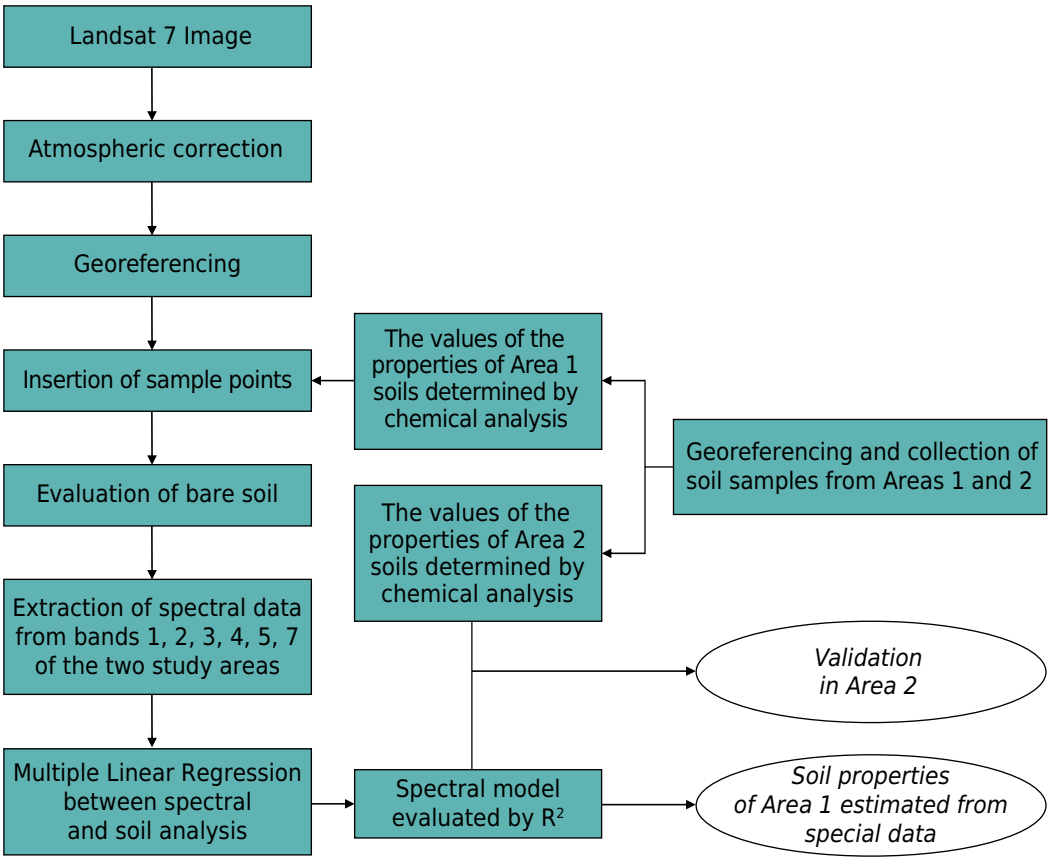

Figure 1. Flow chart with main steps adopted in the present study to quantify the soil particle size.

Soil collection and analysis

To calibrate the model in Area 1, 514 soil sampling points were collected for texture estimation, and 729 sampling points were used in Area 2 for model extrapolation, considering the 0.00-0.20 m surface layer. Particle size was determined by the hydrometer method, using sodium hexametaphosphate as a dispersant (Camargo et al., 1987), quantifying the sand, silt, and clay fractions (Table 1).

The texture classes considered were sandy (clay content <150 g kg^{-1}), sandy loam (clay content 150 – 250 g kg^{-1}), clayey loam (clay content 250 – 350 g kg^{-1}), clayey (clay content 350 – 600 g kg^{-1}), and very clayey (clay content >600 g kg^{-1}) soil, since weathered soils, common in tropical regions (humid and hot climate), are little influenced by silt content.

Acquisition of images and spectral data

The bare soil mask was created according to the methodology developed by Fongaro (2015). The software used for atmospheric correction and data processing was ENVI 5.1. We used 38 images from Landsat 7 ETM^{+}, orbit/point 220/75 (Area 1) and 224/72 (Area 2), using multispectral bands B1 (0.45 to 0.52 µm), B2 (0.52 to 0.60 µm), B3 (0.63 to 0.69 µm), B4 (0.76 to 0.90 µm), B5 (1.55 to 1.75 µm), and B7 (2.08 to 2.35 µm), but not B6, which is the thermal band.

Since sugarcane crops are predominant in both regions, the selected images corresponded to the period from June to October, when the soil is bare for field renovation. The Landsat 7 satellite was chosen due to the greater number of images containing bare soil from 1999 to 2011. The images obtained from the platform of the United States Geological Survey (USGS) were corrected for atmospheric variations through FLAASH (Fast Line-of-Sight Atmospheric Analysis of Hypercubes) and data in digital numbers were transformed to radiance and then to reflectance.

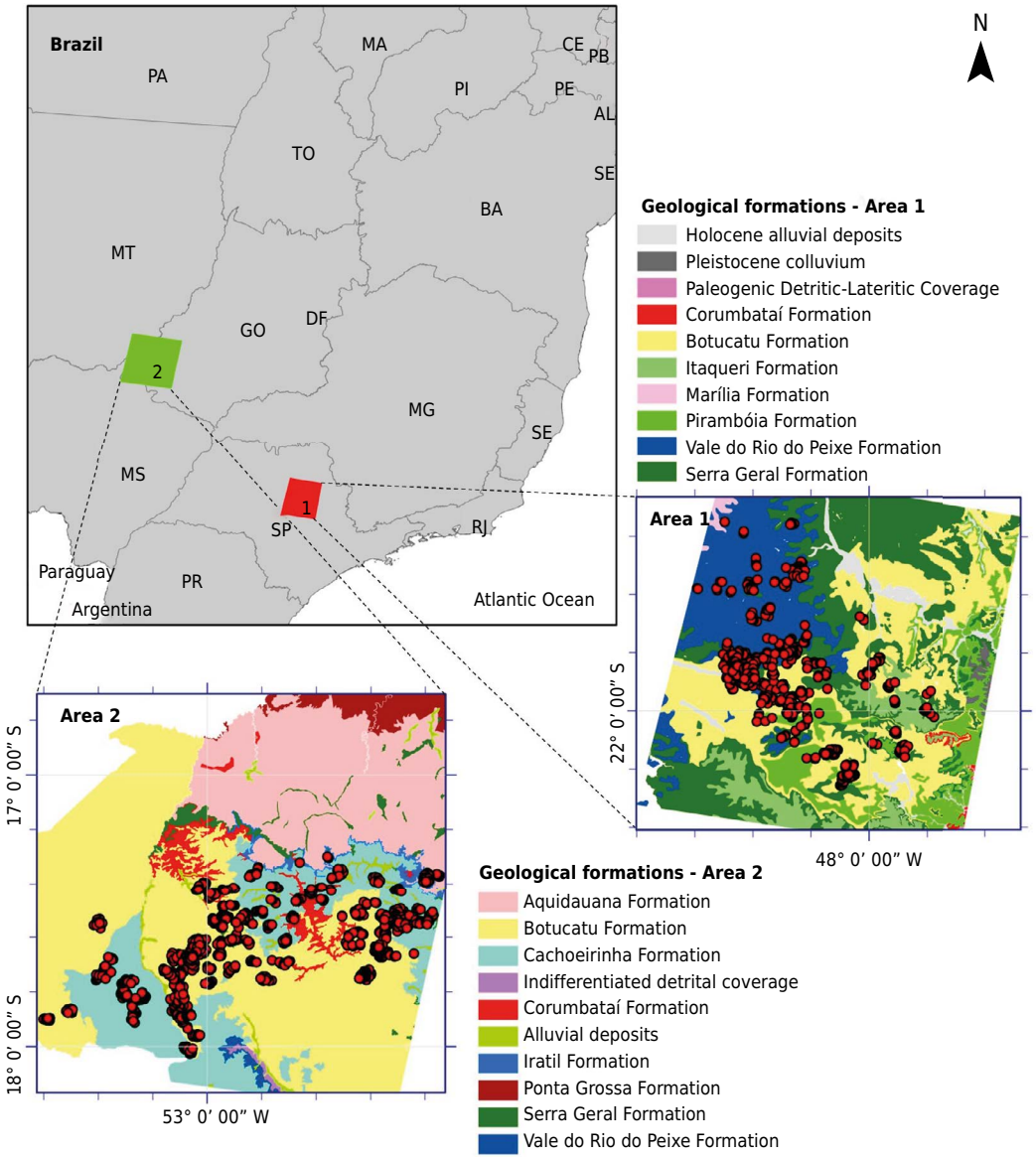

Figure 2. Location of study areas in Brazil and detail of areas, showing local geology and distribution of sampling points (in red).

Table 1. Descriptive statistics of soil contents of clay, sand, and silt in Area 1 and 2

Soil Particle Analysis[(1)]	Sand	Silt	Clay
		Area 1	
No. of observations	514	514	514
Minimum (g kg^{-1})	86.00	0.00	8.00
Maximum (g kg^{-1})	968.00	347.00	643.00
Mean (g kg^{-1})	709.39	62.49	228.10
Coefficient of variation (%)	0.28	1.01	0.65
		Area 2	
No. of observations	729	729	729
Minimum (g kg^{-1})	66.00	11.00	25.00
Maximum (g kg^{-1})	960.00	279.00	879.00
Mean (g kg^{-1})	678.76	49.22	272.19
Coefficient of variation (%)	0.40	0.89	0.89

[(1)] Particle size was determined by the hydrometer method, using sodium hexametaphosphate as a dispersant.

Vegetation was eliminated from the images using the Normalized Difference Vegetation Index (NDVI) (Equation 1). Pixels with values greater than 0.25 were considered as vegetation, and this threshold was pre-established in the ENVI 5.1 software used to eliminate vegetation from the images. To eliminate crop residue, we used the ratio between shortwave infrared bands (IVI) (Equation 2), as proposed by Madeira Netto (1991). Areas that had values above 0.15 were removed from the image (Fongaro, 2015).

$$NDVI = \frac{B4 - B3}{B4 + B3} \quad \text{Eq. 1}$$

$$IVI = \frac{B5 - B7}{B5 + B7} \quad \text{Eq. 2}$$

The soil shows ascending behavior in bands B1, B2, and B3 (Demattê et al., 2015) and, therefore, we used subtractions B2 - B1 and B3 - B2 to remove the pixels that exhibited descending behavior (negative values). Visual assessment was made using the false-color composition 5, 4, and 3, representing the bands red (R), green (G), and blue (B), respectively. In ENVI 5.1, after 5 % enhancement, the areas of bare soil exhibited purple color for clayey soils and tended to pinkish for sandy soils. The raster package (Hijmans, 2015) in R (R Development Core Team, 2017) was used to combine the images into a single bare soil image. The bare soil mask of Area 1 and the GPS sampling points were inserted into ArcGis 10.3. Applying the Extract Multi Values to Point function, reflectance values were extracted from the images of the study site. Null values were disregarded, indicating that the sampling point was in a region of the image that did not represent bare soil. A table containing reflectance, sampling points, and particle size values were included in R (R Development Core Team, 2017) to create the model.

Model creation and validation

Multiple linear regression models were developed in R to estimate the particle size values for Area 1, using six spectral bands and 70 % of sampling points of the surface layer (0.00-0.20 m) (Equation 3). Only the most important independent variables were inserted into the model, selected from the metric RMSE obtained from the Cubist package (Kunh et al., 2017).

$$C = b0 + b1 \times L1 + b2 \times L2 + ... + bn \times Ln \quad \text{Eq. 3}$$

in which C refers to texture, b0 is the intercept, and b1, b2, ..., bn are the weighting factors for the spectra read at several selected wavelengths from 1 to n; L1, L2, ..., Ln indicates the spectral parameter values for the wavelengths from 1 to n, representing the reflectance data. To observe the capacity of model prediction, prevalidation of the model was conducted with 30 % of the remaining sampling points of the same area, chosen at random.

The bare soil image in Area 2 was created and the reflectance values were extracted for texture prediction. Model extrapolation was evaluated by the R^2 and RMSE between the estimated values and those determined by the physical-chemical analysis of the samples.

RESULTS AND DISCUSSION

Bare soil mask

One of the difficulties of working with satellite image data is not being certain of which locations are bare soil. Therefore, the methodology developed by Fongaro (2015), allowed bare soil areas to be established with greater certainty, facilitated by creating masks that removed reflectance data other than from bare soil. The method allowed 43 % bare soil utilization in both Areas 1 and 2 (Figure 3b), while a single image allowed only 16 % in Area 1 and 28 % in Area 2. In Area 2, depending on the year, the soil was completely covered by vegetation (Figure 3a).

There was a well-defined distinction between regions of sandy and clayey texture (Figure 3c). The presence of different clay minerals and particle size distributions influenced the spectral response of soils (Meneses and Madeira Netto, 2001). Thus, soils with sandy texture, dominated by quartz and that contain low levels of iron oxides, tended to have greater reflectance intensity compared to clayey soils (Resende et al., 2005). Even in satellite images with a spatial resolution of 30 m, wide spectral bands, and sensor at a distance of approximately 700 km from the target, bands 5 and 7 discriminated textural classes of the soil surface layer (0.00-0.20 m) well, mainly because a good bare soil mask had been constructed (Figure 3d, Figures 4a and 4b). No reliable differentiation between textural classes by spectral bands indicates that the model to be generated will not perform well.

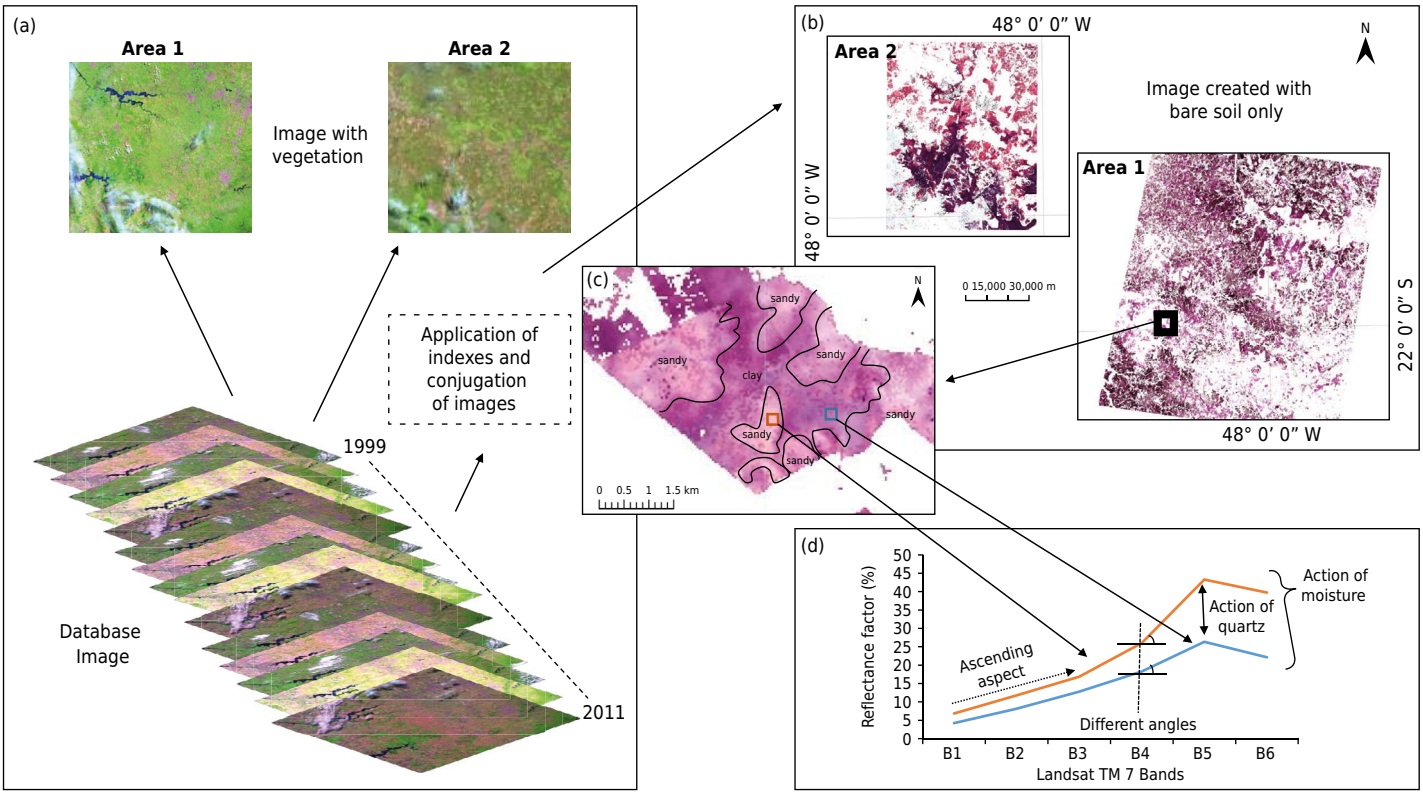

Figure 3. Simulation of the database image used in construction of the bare soil mask. There are images with maximum plant cover (a); the bare soil mask of the two study areas (b); detail of an exposed soil region in which it is possible to differentiate sandy and clayey areas (c); point spectral response of the pixel taken from the sandy and clayey region (d).

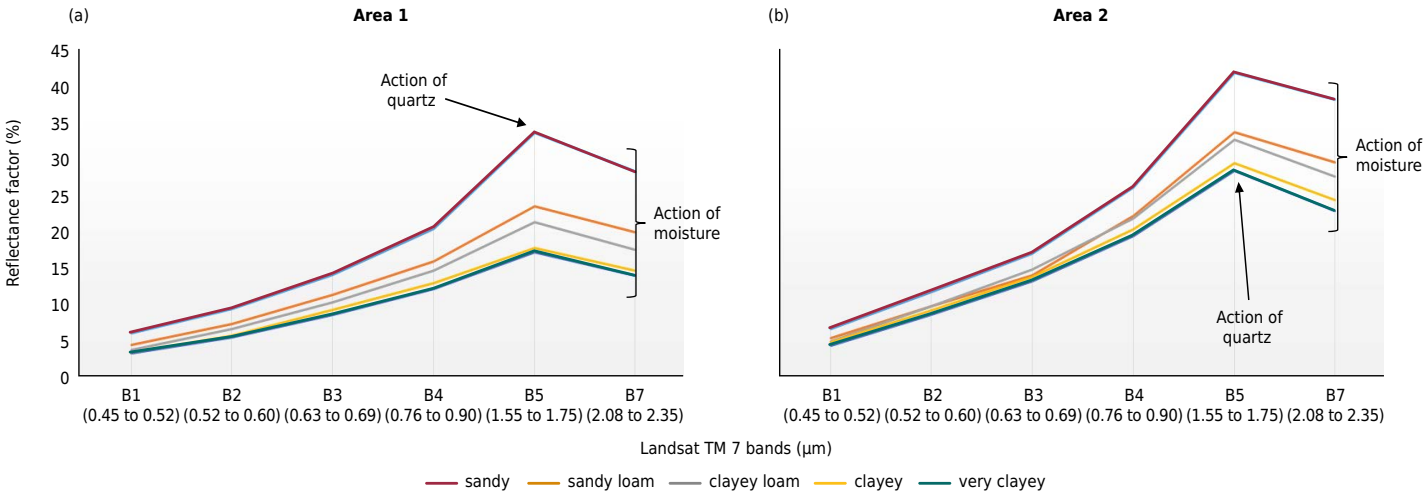

Figure 4. Spectral mean values of the textural classes obtained from the Landsat ETM$^+$ bands.

The difference in color intensity represents the spatial variations of soil texture (Figure 3c). In the false-color composition (RGB - bands 543), applied in the current study, the spectral responses of clayey textures exhibited darker shades of purple color, and pinkish tones appeared for sandy textures. Furthermore, the strategy of evaluating a single pixel for all the bands can be applied to differentiate soil texture as well, from which the spectral curve was extracted. The spectral curve was used to perform a local (point) evaluation and the image was used for spatial (general) analysis. Point analysis showed differences between the spectra of sandy and clayey textures. Sandy soils showed an upward curve, an angle with greater inclination between B4 and B5, and greater intensity between B5 and B7 (Figure 3d). The user can therefore choose the strategy for soil evaluation.

The mean spectral curves according to the textural classes are presented in figures 4a and 4b. In general, from clayey to sandy soils, there are changes in the albedo and in the ascending behavior. Bands 5 and 7 were the most evident in discriminating soils, explained by the performance of quartz within this range (Resende et al., 2005). The curve sequence also performed consistently because as the clay content decreased and the sand content increased, the reflectance in B5 and B7 increased. The B5 and B7 bands correspond to wavelengths 1.55-1.75 and 2.08-2.35 µm, respectively. Within these spectral ranges, electromagnetic energy absorption occurs due to vibrational processes of water molecules and Al-OH in the structures of minerals. Thus, sandy soils that retain less water and contain more simplified mineralogy, such as quartz, exhibit higher reflectance in these wavelengths than a clayey soil that retains more water and contains clay minerals with structural water.

Soil texture estimated by multiple linear regression

Sand and clay were the particle size fractions used to develop the models. In a study performed by Demattê et al. (2007), it was observed that the silt fraction had low correlation with the TM bands (Landsat 5) and it was not used for prediction. Clay had the highest negative correlation coefficients for all bands, with values from -0.68 to -0.72 in bands 5 and 7. The sand fraction had a lower correlation with band 1 of Landsat 7 ETM$^+$ and higher positive values for all other bands analyzed (Table 2). A correlation of -0.40 for clay was obtained by Henderson et al. (1992) when the methods for identifying bare soil in satellite images had not yet advanced. Currently, the development of RS technologies has allowed greater interaction of soil properties like texture with electromagnetic energy to be captured, increasing the correlation values. Lower correlations occurred in B1, B2, and B3 because of less interaction of electromagnetic energy with soil texture and greater interaction of energy with other soil components that show specific spectral responses in these wavelengths (Barnes and Baker, 2000).

In Area 1, the MLR models exhibited R^2 values of 0.64 for clay and 0.63 for sand in validation (Table 3). Correlation analysis between determined and estimated values for clay and sand properties are shown in figures 5a and 5b. Values of R^2 between 0.50 and

Table 2. Pearson correlation between the soil particle analysis and the mean soil reflectance of area 1

Property	Landsat 7 ETM$^+$ Bands					
	B1 (0.45-0.52 µm)	B2 (0.50-0.60 µm)	B3 (0.63-0.69 µm)	B4 (0.76-0.90 µm)	B5 (1.55-1.75 µm)	B7 (2.08-2.35 µm)
Clay	-0.50	-0.59	-0.61	-0.65	-0.68	-0.72
Sand	0.48	0.57	0.60	0.63	0.67	0.70

Significant correlation at the level of 1 %.

Table 3. Results obtained in validation of multiple linear regression elaborated from the soil reflectance of area 1 obtained at orbital level

Property	Multiple equation[(1)]	RMSE	R^2
		%	
Clay	281 - 13 B7 + 9.4 B3 + 1.1 B5	9.24	0.64
Sand	585.5 + 29.5 B7 – 12.8 B5 – 5.3 B3	12.85	0.63

Significant correlation at the level of 1 %. [(1)] Landsat 7 ETM$^+$ bands: B1, B2, B3, B4, B5, B7.

0.65 indicate the possibility of discriminating high and low contents in the model (Saeys et al., 2005). Similar results were found by Demattê et al. (2007) using the Landsat 5 TM sensor, with R^2 values of 0.36 and 0.67 for clay and sand, respectively. Sousa Júnior et al. (2011) quantified soil properties using the Aster sensor and found lower values for clay (0.34) and sand (0.41) than those found in this study.

Most studies that used MLR models with spectral laboratory data to predict clay showed R^2 values ranging from 0.44 to 0.95, with predominance of values above 0.60. In the case of MLR models with satellite data, R^2 values for clay ranged from 0.40 to 0.71 (Table 4). These findings corroborate the R^2 values determined in the current study with the use of a satellite sensor with six bands and spatial resolution of 30 m. This fact also shows that an R^2 value of 0.70 can be considered a limit for the conditions of multispectral satellite sensors, since laboratory sensors with 1,500 bands and spatial resolution of 2 cm^2 obtained R^2 values above 0.70 (Table 4).

Model extrapolation

When applying the model from Area 1 to Area 2, there was a high correlation between the determined and estimated values of clay and sand properties (Figures 6a and 6b), which was similar to the values found for Area 1. The quantification of soil properties by a satellite sensor with six bands is a difficult task, due to soil complexity (Demattê et al., 2007). Therefore, R^2 values above 0.60 can be considered a suitable result, allowing the model to be used in other crop fields.

The RMSE obtained from the validation model generated in Area 2 was 26.78 % for clay and 28.43 % for sand, much higher than the RMSE found for the model applied in Area 1 (9.24 % for clay and 12.85 % for sand, Table 3). This may be due to the contrasts in particle size levels observed in both areas (Table 1). The sampling points in Area 1 are distributed over four geological formations, with three composed of sedimentary rocks, such as sandstones (Formations of Rio do Peixe Valley, Botucatu, and Pirambóia), and one composed of igneous rock, such as diabase (Serra Geral Formation). The weathering and pedogenesis of sandstones give rise to sandy soils, with maximum sand contents of 969 g kg^{-1}, while diabases give rise to more clayey soils, with the highest clay contents of 619 g kg^{-1} (Figure 2 and Table 1a).

The sampling points in Area 2 are distributed on the Cachoeirinha Formation, composed of clayey sedimentary material, and Botucatu Formation, composed of sandy sedimentary rocks (Figure 2). Soils developed from the first formation have clayey texture, with a maximum clay content of 879 g kg^{-1}, while soils developed from the second formation are sandy, with sand content similar to that of Area 1 (maximum of 960 g kg^{-1}) (Table 1b). The larger clay contents in Area 2 are outside of the data range of the model constructed in Area 1, and this implies inaccuracy of estimates by MLR for Area 2.

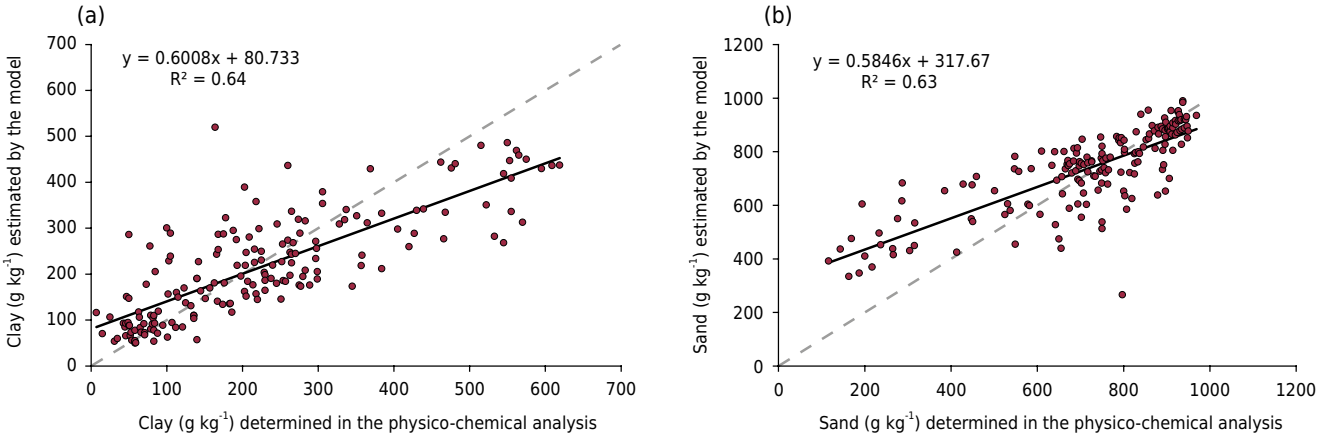

Figure 5. Coefficient of determination of the soil properties of Area 1 estimated by the equations generated from the reflectance data of the Landsat 7 sensor from the same area. The dotted line represents the ideal model.

Table 4. R^2 values of validation of the sand and clay quantification models by multiple linear regression

Author	Year	Equipment	Data acquisition platform	Sand	Clay
				R^2 Validation	
Coleman et al.	1991	MMR	Laboratory	*	0.63
Coleman et al.	1993	Landsat 5 TM	Orbital	0.14	0.40
Palacios-Orueta and Ustin	1998	Cary 5E spectrophotometer	Laboratory	0.23	0.44
Chang et al.	2001	Perstrop NIR Systems 6500 scanning monochromator	Laboratory	0.82	0.67
Shepherd and Walsh	2002	Espectroradiômetro FieldSpec FR	Laboratory	0.76	0.78
Sørensen and Dalsgaard	2005	NIRSystems 6500	Laboratory	0.80	0.95
Sullivan et al.	2005	Ikonos	Orbital	*	0.55
Nanni and Demattê	2006	IRIS	Laboratory	0.63	0.81
Viscarra-Rossel et al.	2006	Varian Cary 500 and BioRad FTS 175 (Spectrometers)	Laboratory	0.75	0.67
Demattê et al.	2007	Landsat 7 ETM	Orbital	0.50	0.61
Fiorio and Demattê	2009	IRIS	Laboratory	0.84	0.83
		Landsat 5 TM	Orbital	0.71	0.71
Sousa Júnior et al.	2011	ASTER	Orbital	0.41	0.34
		FieldSpec Spectroradiometer	Laboratory	0.53	0.69
Summers et al.	2011	ASD FieldSpec Pro spectroradiometer	Laboratory	*	0.66
Ferraresi et al.	2012	Perkin Elmer Spectrum 100	Laboratory	0.80	0.86
		Varian 600-IR	Laboratory	0.85	0.86
Casa et al.	2013	Field Spec Fr Pro spectroradiometer	Laboratory	0.81	0.76
		MIVIS	Aerial	0.81	0.78
		CHRIS-PROBA	Orbital	0.63	0.62
Garfagnoli et al.	2013	SIM-GA	Aerial	-	0.59
Curcio et al.	2013	ASD FieldSpec Pro spectroradiometer	Laboratory	0.80	0.87
Nawar et al.	2016	FieldSpec-FR	Laboratory	*	0.90
Chagas et al.	2016	Landsat 5 TM	Orbital	0.63	0.56
Castaldi et al.	2016	Field Spec Fr Pro spectroradiometer	Laboratory	0.69	0.71
		EO-1 ALI	Orbital	0.44	0.52
		Sentinel-2 MSI	Orbital	0.60	0.61
		LANDSAT 8 OLI	Orbital	0.17	0.43
		Hyperion	Orbital	0.67	0.58
		EnMAP	Orbital	0.69	0.56
		PRISMA	Orbital	0.67	0.58
		HyspIRI	Orbital	0.66	0.56

* We used the criterion of highest value of R^2 found in data validation.

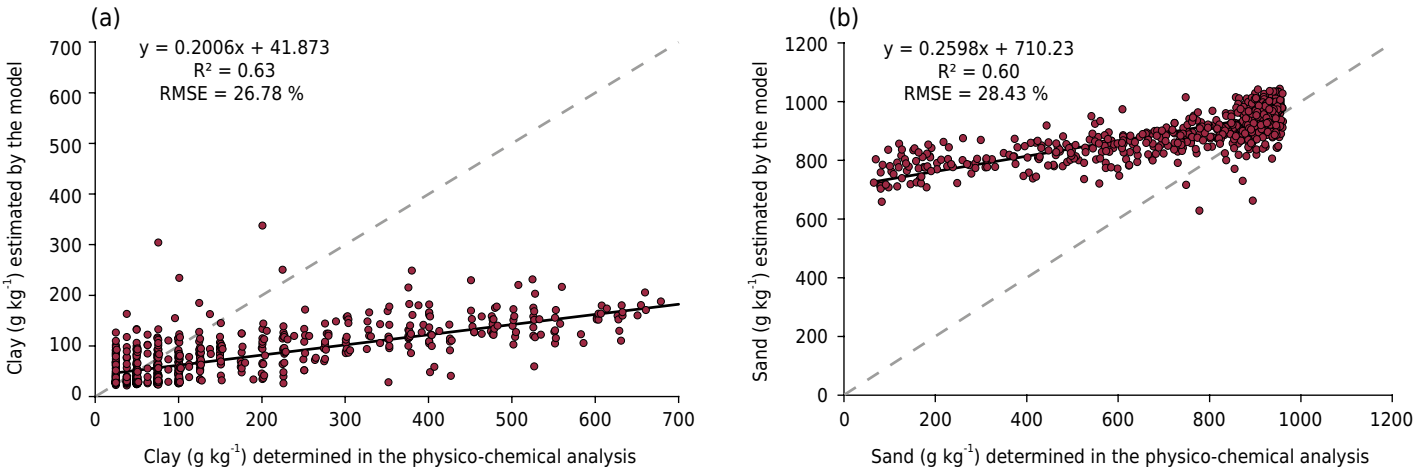

Figure 6. Coefficient of determination of the soil properties of Area 2 estimated by the equations generated from the reflectance data of the Landsat 7 sensor from Area 1. The dotted line represents the ideal model.

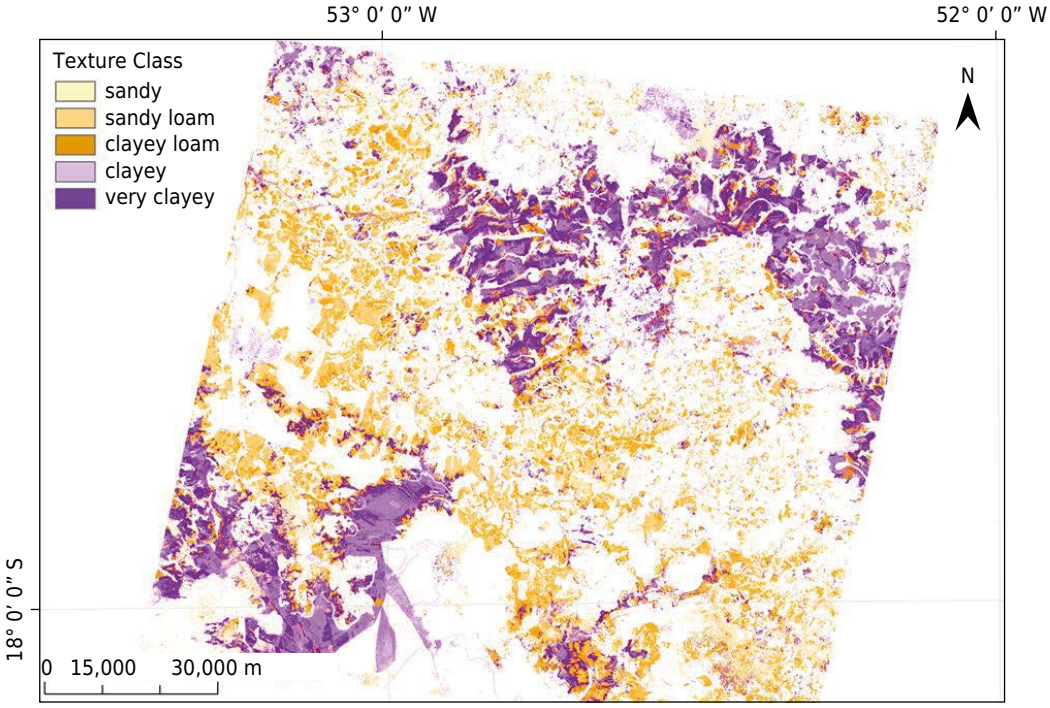

Figure 7. Map of texture classes of Area 2.

However, such distinctions did not substantially interfere with the correlation between sensor bands and soil particle size analysis, demonstrating that the model created for texture quantification may be applied to other areas and also showed good performance for sandy to medium textures. From this model, a prediction map of soil surface texture (Figure 7) was created for Area 2.

Information on the soil textural class assists in soil classification. Although a soil is classified by its B Horizon (which is not detected by the image), a texture map of the soil surface layer may assist in detecting changes in mapping units. This map can be inserted into the precision agriculture system to detect production changes, help create the sampling grid, estimate some physical and hydrological properties of the surface layer, and increase crop yield, among other applications. In this context, spectroscopy techniques are essential for soil management as they generate information quickly and in a less costly manner for agricultural development.

CONCLUSIONS

The method using a mask to remove everything in a satellite image that is not bare soil was successful. The bare soil from a multi-temporal study with satellite images allowed a high percentage of pixels to be indicated as soil, improving the estimation of texture by spectral response with six bands.

It was possible to develop a model for quantification of texture using data from one geographic area that could be applied to a different region, showing less than 13 % error in validation within the calibration area, and less than 30 % error in prediction for an external area.

Bands 5 (1.55-1.75 µm) and 7 (2.08-2.35 µm) were the most significant in clay quantification, reaching correlation values near or greater than 0.70.

It should be emphasized that although the models were successful in the current study areas, they must always be tested in new areas.

REFERENCES

Alves MR. Múltiplas técnicas no mapeamento digital de solos [tese]. Piracicaba: Escola Superior de Agricultura "Luiz de Queiroz"; 2008.

Barnes EM, Baker MG. Multispectral data for mapping soil texture: possibilities and limitations. Appl Eng Agric. 2000;16:731-41. https://doi.org/10.13031/2013.5370

Ben-Dor E, Banin A. Quantitative analysis of convolved TM spectra of soils in the visible, near infrared and short-wave infrared spectral regions (0.4-2.5mm). Int J Remote Sens. 1995;16:3509-28. https://doi.org/10.1080/01431169508954643

Ben-Gera I, Norris KH. Determination of moisture content in soybeans by direct spectrophotometry. Isr J Agric Res. 1968;18:124-32.

Brady NC, Weil RR. Elementos da natureza e propriedades do solo. 3. ed. Porto Alegre: Bookman; 2013.

Camargo MN, Klant E, Kauffman JH. Classificação de solos usada em levantamentos pedológicos no Brasil. Boletim Informativo da Sociedade Brasileira de Ciência do Solo. 1987;12:11-3.

Casa R, Castaldi F, Pascucci S, Palombo A, Pignatti S. A comparison of sensor resolution and calibration strategies for soil texture estimation from hyperspectral remote sensing. Geoderma. 2013;197-8:17-26. https://doi.org/10.1016/j.geoderma.2012.12.016

Castaldi F, Palombo A, Santini F, Pascucci S, Pignatti S, Casa R. Evaluation of the potential of the current and forthcoming multispectral and hyperspectral imagers to estimate soil texture and organic carbon. Remote Sens Environ. 2016;179:54-65. https://doi.org/10.1016/j.rse.2016.03.025

Chagas CS, Carvalho Junior W, Bhering SB, Calderano Filho B. Spatial prediction of soil surface texture in a semiarid region using random forest and multiple linear regressions. Catena. 2016;139:232-40. https://doi.org/10.1016/j.catena.2016.01.001

Chakraborty K, Mistri B. Importance of soil texture in sustenance of agriculture: a study in Burdwan-I C. D. Block, Burdwan, West Bengal. Eastern Geographer. 2015;21:475-82.

Chang C-W, Laird DA, Mausbach MJ, Hurburgh Jr CR. Near-infrared reflectance spectroscopy-principal components regression analyses of soil properties. Soil Sci Soc Am J. 2001;65:480-90. https://doi.org/10.2136/sssaj2001.652480x

Coleman TL, Agbu PA, Montgomery OL. Spectral differentiation of surface soils and soil properties: is it possible from space platforms? Soil Sci. 1993;155:283-93. https://doi.org/10.1097/00010694-199304000-00007

Coleman TL, Agbu PA, Montgomery OL, Gao T, Prasad S. Spectral band selection for quantifying selected properties in highly weathered soils. Soil Sci. 1991;151:355-61. https://doi.org/10.1097/00010694-199105000-00005

Companhia de Pesquisa de Recursos Minerais - CPRM. Mapa geológico do estado de São Paulo. Escala: 1:750.000. São Paulo: CPRM - Serviço Geológico do Brasil; 2006.

Companhia de Pesquisa de Recursos Minerais - CPRM. Mapa geológico do estado do Mato Grosso. Escala: 1:1.000.000. Cuiabá: CPRM - Serviço Geológico do Brasil; 2004.

Curcio D, Ciraolo G, D'Asaro F, Minacapilli M. Prediction of soil texture distributions using VNIR-SWIR reflectance spectroscopy. Procedia Environ Sci. 2013;19:494-503. https://doi.org/10.1016/j.proenv.2013.06.056

Demattê JAM, Alves MR, Terra FS, Bosquilia RWD, Fongaro CT, Barros PPS. Is it possible to classify topsoil texture using a sensor located 800 km away from the surface? Rev Bras Cienc Solo. 2016;40:e0150335. https://doi.org/10.1590/18069657rbcs20150335

Demattê JAM, Araújo SR, Fiorio PR, Fongaro CT, Nanni MR. Espectroscopia VIS-NIR-SWIR na avaliação de solos ao longo de uma topossequência em Piracicaba (SP). Rev Cienc Agron. 2015b;46:679-88. https://doi.org/10.5935/1806-6690.20150054

Demattê JAM, Fiorio PR, Ben-Dor E. Estimation of soil properties by orbital and laboratory reflectance means and its relation with soil classification. The Open Remote Sensing Journal. 2009;2:12-23. https://doi.org/10.2174/187541390100201012

Demattê JAM, Galdos MV, Guimarães RV, Genú AM, Nanni MR, Zullo Junior J. Quantification of tropical soil attributes from ETM +/ LANDSAT-7 data. Int J Remote Sens. 2007;28:3813-29. https://doi.org/10.1080/01431160601121469

Feizizadeh B, Blaschke T. Land suitability analysis for Tabriz County, Iran: a multi-criteria evaluation approach using GIS. J Environ Plann Man. 2013;56:1-23. https://doi.org/10.1080/09640568.2011.646964

Ferraresi TM, Silva WTL, Matin-Neto L, Silveira PM, Madari BE. Espectroscopia de infravermelho na determinação da textura do solo. Rev Bras Cienc Solo. 2012;36:1769-77. https://doi.org/10.1590/S0100-06832012000600010

Fiorio PR, Demattê JAM. Orbital and laboratory spectral data to optimize soil analysis. Sci Agric. 2009;66:250-7. https://doi.org/10.1590/S0103-90162009000200015

Foley JA, DeFries R, Asner GP, Barford C, Bonan G, Carpenter SR, Chapin FS, Coe MT, Daily GC, Gibbs HK, Helkowski JH, Holloway T, Howard EA, Kucharik CJ, Monfreda C, Patz JA, Prentice IC, Ramankutty N, Snyder PK. Global consequences of land use. Science. 2005;309:570-4. https://doi.org/10.1126/science.1111772

Fongaro CT. Mapeamento granulométrico do solo via imagens de satélite e atributos de relevo [dissertação]. Piracicaba: Escola Superior de Agricultura "Luiz de Queiroz"; 2015.

Garfagnoli F, Ciampalini A, Moretti S, Chiarantini L, Vettori S. Quantitative mapping of clay minerals using airborne imaging spectroscopy: new data on Mugello (Italy) from SIM-GA prototypal sensor. Eur J Remote Sens. 2013;46:1-17. https://doi.org/10.5721/EuJRS20134601

Henderson TL, Baumgardner MF, Franzmeier DP, Stott DE, Coster DC. High dimensional reflectance analysis of soil organic matter. Soil Sci Soc Am J. 1992;56:865-72. https://doi.org/10.2136/sssaj1992.03615995005600030031x

Hijmans RJ, Philips S, Leathwick J, Elth J. Dismo species distribution modeling. R package version 1.0-12. Vienna: The R Foundation for Statistical Computing; 2015. Available from: http://cran. R-project.org

Hristov B. The importance of soil texture in soil classification systems. Journal of Balkan Ecology. 2013;16:137-9.

IUSS Working Group WRB. World reference base for soil resources 2014, update 2015: International soil classification system for naming soils and creating legends for soil maps. Rome: Food and Agriculture Organization of the United Nations; 2015. (World Soil Resources Reports, 106).

Kunh M, Steve W, Chris K, Nathan C, Quinlan R. Package 'Cubist'. Version 0.2.1. 2017. https://topepo.github.io/Cubist

Li X-Y, Ma Y-J, Xu H-Y, Wang J-H, Zhang D-S. Impact of land use and land cover change on environmental degradation in lake Qinghai watershed, northeast Qinghai- Tibet Plateau. Land Degrad Dev. 2009;20:69-83. https://doi.org/10.1002/ldr.885

Liao K, Xu S, Wu J, Zhu Q. Spatial estimation of surface soil texture using remote sensing data. Soil Sci Plant Nutr. 2013;59:488-500. https://doi.org/10.1080/00380768.2013.802643

Madeira Netto JS. Étude quantitative des relations constituants minéralogiquesréflectance diffuse des latosols Brésiliens [tese]. Paris: Université Pierre et Marie Curie, 1991.

Meneses PR, Madeira Netto JS. Sensoriamento remoto- reflectância dos alvos naturais. Brasília, DF: Universidade de Brasília; 2001.

Nanni MR, Demattê JAM. Spectral reflectance methodology in comparison to traditional soil analysis. Soil Sci Soc Am J. 2006;70:393-407. https://doi.org/10.2136/sssaj2003.0285

Nawar S, Buddenbaum H, Hill J, Kozak J, Mouazen AM. Estimating the soil clay content and organic matter by means of different calibration methods of vis-NIR diffuse reflectance spectroscopy. Soil Till Res. 2016;155:510-22. https://doi.org/10.1016/j.still.2015.07.021

Okparanma RN, Mouazen AM. Determination of total petroleum hydrocarbon (TPH) and polycyclic aromatic hydrocarbon (PAH) in soils: a review of spectroscopic and non-spectroscopic techniques. Appl Spectro Rev. 2013;48:458-86. https://doi.org/10.1080/05704928.2012.736048

Palacios-Orueta A, Ustin SL. Remote sensing of soil properties in the Santa Monica Mountains I. Spectral analysis. Remote Sens Environ. 1998;65:170-83. https://doi.org/10.1016/S0034-4257(98)00024-8

R Development Core Team. R: A language and environment for statistical computing. R Foundation for Statistical Computing, Vienna, Austria; 2017 [accessed on 2016 Feb 14]. Available from: https://www.R-project.org/.

Resende M, Curi N, Ker JC, Rezende SB. Mineralogia de solos brasileiros: interpretação e aplicações. Lavras: Editora UFLA; 2005.

Rolim GS, Camarago MBP, Lania DG, Moraes JFL. Classificação climática de Köppen e de Thornthwaite e sua aplicabilidade na determinação de zonas agroclimáticas para o estado de São Paulo. Brangantia. 2007;66:711-20. https://doi.org/10.1590/S0006-87052007000400022

Saeys W, Mouazen AM, Ramon H. Potential for onsite and online analysis of pig manure using visible and near infrared reflectance spectroscopy. Biosyst Eng. 2005;91:393-402. https://doi.org/10.1016/j.biosystemseng.2005.05.001

Shepherd KD, Walsh MG. Development of reflectance spectral libraries for characterization of soil properties. Soil Sci Soc Am J. 2002;66:988-98. https://doi.org/10.2136/sssaj2002.9880

Sistema Estadual de Geoinformação do Estado de Goiás - SIEG [internet]. Goiânia: 2013 [acesso em 09 mar 2018]. Disponível em: http://www2.sieg.go.gov.br/post/ver/171319.

Sørensen LK, Dalsgaard S. Determination clay and other soil properties by near infrared spectroscopy. Soil Sci Soc Am J. 2005;69:159-67. https://doi.org/10.2136/sssaj2005.0159

Sousa Júnior JG, Demattê JAM, Araújo SR. Modelos espectrais terrestres e orbitais na determinação de teores de atributos dos solos: potencial e custos. Bragantia. 2011;70:610-21. https://doi.org/10.1590/S0006-87052011000300017

Sullivan DG, Shaw JN, Rickman D. IKONOS imagery to estimate surface soil property variability in two Alabama physiographies. Soil Sci Soc Am J. 2005;69:1789-98. https://doi.org/10.2136/sssaj2005.0071

Summers D, Lewis M, Ostendorf B, Chittleborough D. Visible near-infrared reflectance spectroscopy as a predictive indicator of soil properties. Ecol Indic. 2011;11:123-31. https://doi.org/10.1016/j.ecolind.2009.05.001

Teixeira PC, Donagemma GK, Fontana A, Teixeira WG. Manual de métodos de análise de solo. 3. ed. rev. ampl. Brasília, DF: Embrapa; 2017.

Viscarra-Rossel RA, Walvoort DJJ, McBratney AB, Janik LJ, Skjemstad JO. Visible, near infrared, mid infrared or combined diffuse reflectance spectroscopy for simultaneous assessment of various soil properties. Geoderma. 2006;131:59-75. https://doi.org/10.1016/j.geoderma.2005.03.007

Zeng DH, Hu YL, Chang SX, Fan ZP. Land cover change effects on soil chemical and biological properties after planting Mongolian pine (*Pinus sylvestris* var. *mongolica*) in sandy lands in Keerqin, northeastern China. Plant Soil. 2009;317:121-33. https://doi.org/10.1007/s11104-008-9793-z